

Mott transitions and Novel Orders in Multi-Orbital Models: The Relevance of Structural “Double Exchange”

Mukul S. Laad¹, S. Koley² and A. Taraphder²

¹ *Institute of Mathematical Sciences, Chennai 600013, India*

² *Department of Physics and Centre for Theoretical studies,
Indian Institute of Technology, Kharagpur 721302 India*

(Dated: August 24, 2021)

In real transition-metal oxides, the so-called GdFeO_3 octahedral tilt is long known to be a relevant control parameter influencing the range of orbital and magnetic ordered states found across families of cubic perovskite families. Their precise role in the interplay between itinerance and localisation, long known to underpin Mottness in d -band oxides, has however received much less attention. We analyse the relevance of the GdFeO_3 tilt in detail in a representative setting of a partially-filled e_g orbital system. We identify a new generalised principle of broad relevance, namely, that this tilt acts like a structural “double exchange” and acts contrary to the well-known Anderson-Hasegawa double exchange. As a function of this tilt, therefore, a phase transition from a Mott-Hubbard insulator to an incoherent bad-metal occurs as an effective band-width-controlled Mott transition. We analyse the incoherent metal in detail by studying one- and two-particle spectral responses and propose that this selective-metal is a novel orbital analogue of the FL^* state with fractionalised *orbitons*. Finally, we apply these ideas to qualitatively discuss the effect of strain on thin films of such d -band oxides on suitable substrates, and discuss the exciting possibility of engineering novel ordered phases, such as unconventional circulating currents, nematics and superconductors, by suitable strain engineering in TMO thin films.

PACS numbers: 72.80.Ga, 71.28+d, 71.10.Ca, 72.10-d

Mott transitions, induced either by bandwidth control or doping¹ are by now believed to underpin novel phenomena in transition metal oxides (TMO). Among many others, occurrence of spectacular phenomena such as unconventional high- T_c superconductivity², colossal magnetoresistance³ and multiferroicity⁴, along with huge changes in response to minute perturbations open up attractive potential for designing new devices where these features can be profitably exploited. On the fundamental side, in multi-orbital systems, additional, interesting physics related to *orbital* selective Mott transition(s) emerges in the intermediate correlation regime⁵. This generically leads to bad-metallic, non-Landau Fermi liquid (nLFL) metallic behavior, topological restructuring of the large Fermi surface (FS) of the LFL, and fractionalisation of elementary excitations⁶, as exemplified in the FL^* idea. Given the multi-band situation intrinsic to most real oxides, these novel features may be more broadly found in TMOs than currently known. In particular, whether an analogous orbital-correlation driven orbital- FL^* (i.e. OFL^*) state with fractionalised (charge neutral) fermionic orbitons can be realised remains completely unexplored, despite proposals for orbitons as analogues of magnons being extant in literature⁷.

In this context, recent proposals to use heterostructuring and orbital engineering in concert with remarkable advances in synthesising artificial layered structures of TMO have provided exciting impetus to attempts to design materials with exotic properties not to be found in the bulk⁸. Various factors, e.g. quantum confinement, interface orbital polarisation due to chemical confinement and epitaxial constraint on crystal symmetry are believed to conspire in selecting specific electronic ground states in

superlattices of TMO. One expects such a wide range of ground states to be selected by “tuning” the system, e.g. by external strain, which can be applied by using appropriately terminated substrates, e.g. a 2.2 percent tensile strain on $\text{LaNiO}_3/\text{LaAlO}_3$ (LNO/LAO) superlattices has been achieved⁹ by using a TiO_2 -terminated (001) SrTiO_3 substrate.

As regards orbital engineering, chemical confinement and epitaxial constraints will modify the interfacial orbital character of electronic states in TMO films relative to their bulk character. Tensile or compressive strain will also produce such changes¹¹, with the added attractive advantage of providing a knob to “continuously” tune the orbital character. In TMO, this must occur as a result of changes in the GdFeO_3 tilt, known to be a ubiquitous feature. More precisely, in corner-sharing TMO_6 octahedra in TM oxides, off-equilibrium displacements of the lighter O ions induces coupled distortions into the problem. This leads to anti-ferrodistortive displacements, resulting from octahedral tilt, the so-called GdFeO_3 distortion. In situations where the one-electron hopping between the TM ions is mediated by the intervening O ions, as in cuprates and manganites, this tilt directly affects wavefunction overlap and degree of itinerance. Since the remarkable responses of TMOs are a direct fall-out of the competition between itinerance and local interactions, the resulting GdFeO_3 tilt angle, θ , turns out to be a relevant “control parameter”, readily tunable by external pressure or uniaxial strain. In cubic ABO_3 perovskites, the A -atom size controls the magnitude of θ , and is known from many studies^{12,13} to be an important feature in evolution of ground states and physical properties as a function of A . Clearly, this globally important feature must also play an

important role in evolution of ground states and physical responses in TMO heterostructures. To the best of our knowledge, how this specific aspect affects the competition between itinerance and Mott localisation in TMO, along with the more fundamental theoretical issues mentioned above, remains to be addressed systematically.

We start by searching for a basic theoretical systematization of the trends found in the better studied cubic ABO₃ systems. Partly, difficulty in achieving this stems from the paucity of well-controlled theoretical tools capable of describing *all* effects (itinerance, local Hubbard interactions, Jahn-Teller (JT) distortions, *GdFeO*₃ tilt) in *real* TMOs in a single picture. An aim of our study is to retain essential aspects of the general problem in a simplified effective model, yet one which should be tractable enough to give a broad applicability and predictive power.

Here, we illustrate how such trends as found experimentally across a wide range of TMO families are rationalized in such a “simple” effective model. Specifically, we consider how major trends above vary with θ . We show that a wide variety of such trends in diverse TMO¹⁴ can be understood directly in terms of a very simple underlying theme, whose derivation and study of consequences is the main result of this work:

The GdFeO₃ tilt in TMOs acts as a “structural double exchange” in the orbital sector. It acts contrary to the well-known Anderson-Hasegawa double exchange (DE), and the competition between these two double exchange processes is at the heart of the unusually rich and complex outcomes observed in experiment as structural features are appropriately tuned.

Building upon these strengths, we apply this theme to study the Mott insulator-to-bad metal transition in a single layer TMO (e.g, manganite) film described by a two-orbital Hubbard model including “realistic” features specific to e_g -orbital systems. Using an effective model for the interface based on DMFT results, we also discuss how novel orders in TMO thin films on suitable substrates can arise via route(s) unanticipated in the case of bulk TMOs. We stress, however, that our model and results have a broad application to TMOs in general, and our results admit an in-principle generalisation to t_{2g} -based TMOs as well.

I. MODEL

Specifically, motivated by intense interest in manganite and nickelate-based thin films¹⁵, we consider a 2D, two-orbital (e_g orbitals) system with the *GdFeO*₃ octahedral distortion, with Hamiltonian,

$$H = H_{band} + H_{int} + H_{JT} \quad (1)$$

where H_{band} consists of the hopping part in the e_g sector, plus the *GdFeO*₃ distortion, and H_{int} is the multi-orbital Coulomb part. Explicitly, $H_{band} =$

$-\sum_{\langle i,j \rangle, a,b} t_{ij}^{ab} (a_{i\sigma}^\dagger b_{j\sigma} + h.c)$ where the t_{ij}^{ab} have very specific orbital dependent structures for the two e_g orbitals in 2D (a, b stand for the two e_g orbitals, e.g., $d_{x^2-y^2}$ and $d_{3z^2-r^2}$ for manganites). The *GdFeO*₃ distortion can be included in t_{ij}^{ab} via an angle, θ , describing the rotation of the *TMO*₆ octahedra. We have $t^{aa} = (3t/4)\cos^3\theta$, and $t^{bb} = (t/4)\cos\theta$, while $t^{ab} = t^{ba} = (\sqrt{3}t/4)\cos^2\theta$ for hopping along y , while $t^{ab} = t^{ba} = (-\sqrt{3}t/4)\cos^2\theta$ for hopping along x . Interestingly, the inter-orbital hopping has an explicit d -wave character with a form-factor ($\cos k_x \cos k_y$) in momentum space, a feature that can facilitate unconventional orbital order, detailed later in this work.

The multi-orbital Coulomb interactions in the d -shell are described by $H_{int} = U \sum_{i,\alpha=a,b} n_{i\alpha\uparrow} n_{i\alpha\downarrow} + U' \sum_i n_{ia} n_{ib} - J_H \sum_i \mathbf{S}_{ia} \cdot \mathbf{S}_{ib}$. Additionally, for partially filled e_g orbitals, the JT distortion lifts the e_g orbital degeneracy at the outset, contributing the well-known term, $H_{JT} = gQ_2 \sum_{i\sigma} (a_{i\sigma}^\dagger b_{i\sigma} + h.c) + gQ_3 \sum_{i\sigma} (n_{i\sigma} - n_{i\bar{\sigma}})$, to the Hamiltonian. Q_2 and Q_3 are the relevant distortions of the lattice (see J. Kanamori¹⁶ for the standard notations and definitions of the Jahn-Teller distortion magnitudes Q_2, Q_3). To simplify matters, we consider *quasi-static* JT distortions to begin with: this seems to be quite adequate for the case of $D = 2$ (bilayer) manganites, as found very recently¹⁷ but it is an approximation. In this limit, the JT term can be written in a manifestly “orbital double-exchange” form³: $H_{J-T} = g \sum_i \mathbf{Q}_i \cdot \mathbf{T}_i$ where $\mathbf{Q} = (Q_2, Q_3)$ and $\mathbf{T} = (T^x, T^z) = ((n_a - n_b)/2, a^\dagger b + b^\dagger a)$.

The band Hamiltonian, H_{band} , is readily diagonalized: we introduce the combinations, $c_{\sigma+} = \sum_{\alpha=e_x, e_y} \frac{\sqrt{3}c_\theta^{3/2} \cdot a_\sigma + c_\theta^{1/2} (-1)^\alpha b_\sigma}{\sqrt{c_\theta(1+3c_\theta^2)}}$ and $c_{\sigma-} = \sum_{\alpha=e_x, e_y} \frac{(-1)^\alpha c_\theta^{1/2} \cdot a_\sigma - \sqrt{3}c_\theta^{3/2} \cdot b_\sigma}{\sqrt{c_\theta(1+3c_\theta^2)}}$ with $c_\theta = \cos\theta$. Here, $(-1)^\alpha = +1, -1$ for $\alpha = e_x, e_y$. The c_\pm now defines new, orthogonal combinations of a, b in the *GdFeO*₃ structure. In $D = 2$ manganites, with $a = d_{x^2-y^2}, b = d_{3z^2-r^2}$, the c_\pm transform like $d_{3x^2-r^2}, d_{3y^2-r^2}$. Quite remarkably, geometric effects allow only the $c_{\sigma+}$ to hop: the $c_{\sigma-}$ remains completely dispersionless as long as no additional distortions are introduced: this feature was also apparently discovered earlier by Ferrari *et al.*¹⁸. In the limit $U \rightarrow \infty$, (as in effective FM Kondo lattice models for manganites in the large- J_H limit¹⁹) the interaction terms can be easily re-expressed in terms of the c_\pm as $H_{int} = U' \sum_{i,\sigma,\sigma'} n_{i\sigma+} n_{i\sigma'-} - J_H \sum_i \mathbf{S}_{i+} \cdot \mathbf{S}_{i-}$ while the hopping part is simply $H_{hop} = (t/4) \sum_{i,\alpha=x,y,\sigma} \gamma_{ij}(\theta_{ij}) (c_{i\sigma+}^\dagger c_{i+\alpha,\sigma+} + h.c)$. Results for the original two-band Hubbard model with d -wave hybridisation are readily obtained by undoing the transformation from a, b to c_+, c_- fermions.

Interestingly enough, this is just the $S = 1/2$ Falicov-Kimball (FK) model, as long as the JT term is neglected, and the hopping is uniform, i.e, when $\gamma_{ij}(\theta_{ij}) = C$, a constant. Otherwise, one has an FK model with bond-dependent hopping, $t_{ij} =$

$t\sqrt{c_{\theta_i}(1+3c_{\theta_i}^2)}\sqrt{c_{\theta_j}(1+3c_{\theta_j}^2)}$. Following this, incorporating a Holstein-like electron-lattice ($e-l$) interaction in our case will obviously further enhance the FK-like nature of our model: the dispersionless $c_{\sigma,-}$ states above will now favor polaron formation, even for much more modest $e-l$ coupling. The dispersive band ($c_{\sigma,+}$) will be moderately narrowed by electron-lattice interaction, and this effect can be subsumed into a renormalised hopping strength in H above. In other words, we do *not* need strong electron-lattice coupling, in accord with experimental indications for cubic manganites²⁰. Geometrical effects leading to drastic reduction in band-width for a subset of orbital states will allow polaron formation even for modest $e-l$ coupling.

The new element in our work is that the one-electron hopping explicitly shows up in the dependence on the GdFeO₃ tilt (θ) in a simple way. Variation of θ will thus lead to a (continuous) variation of $U/t(\theta), U'/t(\theta)$ in our FKM, whence the exciting new possibility of a Mott transition driven by octahedral tilt reveals itself in the form of a bandwidth-controlled Mott transition. In the rest of this work, we will use multi-orbital DMFT to solve H and discuss the interesting manifestations of this effect in the cases outlined in the introduction.

II. GdFeO₃-TILT-INDUCED MOTT TRANSITION

Many interesting trends in ground states and physical responses are now readily manifest. To this end, it is helpful to look at a generic situation, which we do by replacing the actual tight-binding DOS for the e_g orbitals above by a simple Bethe lattice DOS. It is known²¹ that the FKM shows a continuous Mott (metal-insulator) transition as $U/zt(\theta)$ is varied through a critical value. For the spinless FKM (corresponding to the saturated half-metal with full ferromagnetic spin polarization due to an effective $J_H = \infty$ ¹⁹) on the Bethe lattice, the critical U' is $U' = 2\sqrt{3}zt(\theta)$ with $t = t(\theta) = t[c_{\theta}(1+3c_{\theta}^2)]$, for $\theta_i = -\theta_j$, corresponding to antiferrodistortive octahedral tilt commonly expected in many TMOs.

Thus, for fixed U' , increasing the GdFeO₃ tilt *reduces* $W(\theta)$, driving a Mott metal-insulator transition as a function of the *tilt angle*, θ ! This can readily be induced by applying pressure, or from coupling to substrate-induced *strain* (see below). Increasing θ also reduces the AF transition temperature: remarkably, at strong coupling, $k_B T_N^{af} \simeq (4t^2/U)$ decreases in tandem with *stabilization* of the Mott insulator. At weak-coupling, $k_B T_N \simeq t(\theta)\exp[-2\pi(\theta)/U]^{1/D}$ within HF-RPA, giving a qualitatively different scaling of $T_N(\theta)$. The orbital ordering scales also follow similar laws, $k_B T_{oo} = (4t^2/U')$ for large U' and $k_B T_{oo} \simeq t(\theta)\exp[-2\pi(\theta)/U']^{1/D}$ for small U' . We thus suggest that studying the pressure or strain dependence of T_N and T_{oo} (by varying the A cation in ABO₃ perovskites) can yield direct information

concerning the degree of electronic correlations (large or small U) and the itinerant vis-a-vis Mottness nature of magnetism in d -band magnetic oxides.

The above is very simply understood by noticing that the GdFeO₃ tilt acts like a “reverse double exchange” - increasing θ reduces $t_{ij}(\theta)$, disfavoring the metallic state and ferromagnetism, but favoring AF-OO Mott insulators. Also, in half-metals, it now turns out that incorporating this *structural* DE into the conventional Anderson-Hasegawa²² argument gives $t_{ij} = t(\theta_{ij})\sqrt{1+(\langle \mathbf{S}_i \cdot \mathbf{S}_j \rangle / 2S^2)}$, revealing the interplay between the structural (reverse, $t(\theta_{ij})$) and conventional DE ($\sqrt{1+(\langle \mathbf{S}_i \cdot \mathbf{S}_j \rangle / 2S^2)}$) in a very transparent way. Incorporation of the all-pervasive structural (GdFeO₃) tilt as a generalized principle, i.e. a “reverse” DE has not been previously realised, to our best knowledge. The major technical advantage of our analysis is thus that such effects can now be easily incorporated into modern correlated electronic structure (LDA+DMFT) approaches as multi-orbital Hubbard models with bond-dependent hoppings.

Clearly, *decreasing* tilt now favors the FM-metal, self-consistently *reducing* the JT distortion via enhanced itinerance. Increasing θ counteracts this tendency, reducing the hopping, favoring OO and JT distorted across the AMO₃ with $M = Ti, Ni$, one should find AF Mott insulators (large θ) giving way to correlated metals (smaller θ) as A is varied: indeed, this fully accords with data, where precisely such a correlation between the magnitude of the GdFeO₃ tilt and evolution of electrical properties (metal or insulator) is known^{12,13}. Further, the “puzzling” weakening of AF order along with stabilisation of the Mott insulator in $RNiO_3$ also falls out rather naturally as discussed above. We emphasise that, in the above, the effective parameters, $t(\theta), U'$ in our FKM include various structural (one-electron bands), chemical (in the effective value of t , reflecting strong covalent $p-d$ overlap in late TMO via $t \simeq t_{pd}^2/\Delta$ where t_{pd} is the one-electron hybridization and $\Delta = (\epsilon_p - \epsilon_d)$ is the charge transfer energy) as well as interaction (U, U', J_H and JT couplings) in a simple effective model. This enabled us to understand global trends in evolution of ordered ground states and electrical properties without explicitly referring to material-dependent microscopic band structural details of specific TMO with partially-filled e_g orbitals. Thus, our derivation of the structural DE and conclusions following from its interplay with conventional DE have a more general validity, as exemplified by good qualitative agreement discussed above.

Thus, we identify the competition between the structural “reverse” DE and conventional DE as the central factor influencing the range of tunable ground states in cubic TMO. However, much work remains to be carried out when one inquires about the role of the above competition in strained thin films (or devices made from sandwiches of such films) involving ABO₃ perovskites, e.g. LSMO/STO²³ or LNO/LAO interfaces²⁴.

III. APPLICATION TO STRAIN-INDUCED MOTT TRANSITION IN TMO THIN FILMS

We now apply the ideas discussed in the introduction and developed in the preceding sections to a very contemporary problem in TMO thin films. Namely, we will consider the following issue, albeit with a simplified model band structure:

Imagine a situation where an atomically thick layer of a TMO, e.g, a manganite or a nickelate, deposited on an appropriately terminated substrate, e.g, (001) face of SrTiO₃ or LaAlO₃ (present advances in technology make this exciting situation possible, and, moreover, the thickness can be varied between one and several TMO layers). In this situation, several new features, not important for bulk TMO, become relevant. The excitement in this field stems from the belief that these allow for additional “knobs” to tune the interplay between various microscopic physical processes, and open the door to engineering desired ground states, which can be further manipulated by small changes in external parameters, i.e, *by slowly turning the knob*. We list these features:

(i) Depending upon the substrate, interfacial strain can be manipulated to be either tensile or compressive. In an e_g -orbital based system, this modifies the multi-orbital one-electron hoppings, as well as the Jahn-Teller splittings. Assuming a (001) growth direction and defining the inlayer strain by $e_{xy} = (a_s - a)/a_s$ with a , a_s the lattice constants of the manganite film and the substrate, $e_{xy} > 0$ (< 0) corresponds to tensile (compressive) strain. The strain along c -axis, $e_z = -4\nu e_{xy}$ with ν being the Poisson ratio. For manganites, we choose $e_z = -3e_{xy}/2$ and $-0.02 \leq e_{xy} \leq 0.02$. This is the same strategy as that employed recently by Baena *et al.*²⁵, and has a number of interesting consequences relevant to our study:

(a) strain modifies the nearest neighbor hopping integral as $t = t(1 - 2e_{xy})$, leading to reduction (enhancement) of itinerance for tensile (compressive) strain.

(b) Tensile strain lowers the on-site energy of the $x^2 - y^2$ orbital (ϵ_1) relative to that of $3z^2 - r^2$, denoted ϵ_2 , while compressive strain does the opposite, i.e, it effectively modifies the magnitude *and* sign of the JT distortion. This effect is modelled by a term, $\sum_{i,\sigma} (\epsilon_1 n_{i,a,\sigma} - \epsilon_2 n_{i,b,\sigma})$ in our original Hamiltonian. Written in terms of the $c_{\sigma,\pm}$, it is exactly of the form of H_{JT} . The important difference is that the *sign* of this *strain induced* “JT”-like distortion can be opposite to that of the usual JT coupling. It is also known that the magnitude of the GdFeO₃ tilt controls (for example, by choosing the A atom in AMnO₃) the magnitude of the usual JT interaction, even for bulk $D = 3$ manganites: the same must then hold for manganite films as well. Also, epitaxial constraints at the interface must lead to octahedral tilts (θ) notably different from their values in the bulk. As we have seen above, this acts like a “reverse” DE, and, by itself, affects the electronic bandwidths and Jahn-Teller splittings, as discussed in detail for the case of bulk AMnO₃. The points (a) and (b) above clearly illustrate how both, the one-electron

hoppings *and* the *net* value of the JT coupling, are rather sensitive to the combined effects of the GdFeO₃ tilt and strain.

(ii) Strong local multi-orbital Coulomb interactions are known to be ubiquitous in TMO, and correlation effects in thin layers are known to be generically enhanced compared to the bulk, due to reduction of screening.

It is very natural to expect that all these features will play an important role when one studies the ground state(s) and associated phase transition(s) between them as tuning parameters like strain or composition are varied. We will consider TMO thin films (e.g, manganite layer on STO substrate) in some detail in this context in what follows. We consider the more realistic *spinful* two-orbital Hubbard model defined in the previous section. Our main focus will be on how the electronic properties of the layer can be sensitively switched by strain engineering, and, in general, by any perturbation which affects the interplay between structural (GdFeO₃ tilt, JT coupling), itinerant (one-electron hoppings via GdFeO₃ tilt) and strong multi-orbital Hubbard interactions. We will also qualitatively discuss their effects on the relative stability of competing magnetic and orbital ordered states, and the broader relevance of our analysis here to other interesting issues that have been the recent focus of attention in TMO heterostructures and thin films.

The two-band Hubbard model for a single-layer, written in terms of the $c_{\sigma,\pm}$ combinations, becomes the spin-1/2 FKM with an additional JT term

$$H_{2D} = \sum_{\langle i,j \rangle, \sigma} t\gamma_{ij}(\mathbf{S})\gamma(\theta_{ij})(c_{i,\sigma,+}^\dagger c_{j,\sigma,+} + h.c) + U \sum_{i,a=\pm} n_{i,a,\uparrow} n_{i,a,\downarrow} + U' \sum_{i,\sigma,\sigma'} n_{i,\sigma,+} n_{i,\sigma',-} + \lambda \sum_i \mathbf{Q}_i \cdot \mathbf{T}_i,$$

as described earlier. The JT coupling is taken to be λ and not g , as before, to signify that this quantity will be renormalised by strain, as discussed above. We re-emphasise that, in our effective $S = 1/2$ FKM, even a modest electron-lattice interaction now drives the system to the anti-adiabatic regime ($\Omega_{ph}/t_- \gg 1$) in the c_- -sector, while, due to a wide band width ($O(2.0)$ eV) of the c_+ , the adiabatic limit is applicable in the latter case. This is intrinsically an orbital-selective electron-lattice coupling, a new feature rigorously demonstrated in our case at the level of a tight-binding band structure (the fact that a very similar tight-binding fit, though with different features, works very well for cubic manganites, at least in the FM metallic phase, was shown earlier and utilised in a DMFT calculation²⁶). Our new effective picture is thus of immobile small polarons in $c_{\sigma,-}$ states co-existing with comparatively wide-band dispersive $c_{\sigma,+}$ electronic states. For the wide (c_+)-sector, the adiabatic limit implies that we may consider the effect of the $\lambda \sum_i \mathbf{Q}_i \cdot \mathbf{T}_i$ term within the quasi-static approximation (neglecting Ω_{ph} , since, in this limit, the Holstein problem reduces to a separate Falicov-Kimball model²⁷), and

this additional FK interaction, $H'_{FK} = u' \sum_{i,\pm} \Delta_i n_{i,c,\pm}$ can be lumped together with the $U' \sum_{i,\sigma,\sigma'} n_{i,\sigma,+} n_{i,\sigma',-}$ in H_{2D} above.

Thus, we are now left with having to analyse the Hamiltonian H_{2D} . Due to the fact that the term $\lambda \sum_i \mathbf{Q}_i \cdot \mathbf{T}_i$ mixes the c_+, c_- states at one-electron level, we have to solve a two-orbital extended Anderson lattice model. To study the questions posed in this work, we solve H_{2D} within multi-orbital dynamical mean field theory (MO-DMFT), using the MO-iterated perturbation theory (MO-IPT) as the impurity solver in DMFT. A wide range of impurity solvers can be used in this context: these range from diagrammatic ones like IPT²⁸, non-crossing approximation (NCA)²⁹, local moment approximation (LMA)³⁰, to numerical exact diagonalisation (ED)³¹, continuous-time quantum Monte Carlo (CT-QMC)³² and numerical renormalization group (NRG)³³. Both approaches yield the correct correlated Landau Fermi liquid (LFL) correlated metallic state and first-order Mott transition in the one-band Hubbard model as well as the selective-Mott transitions accompanied by bad-metallic incoherent non-LFL metallic states in correlated multi-band systems^{34,35}, though, to our knowledge, only NRG achieves the necessary accuracy required to extract the (almost) exact Kondo scale. Diagrammatic approaches have the advantage of being relatively easy to implement, and work at all temperatures: these advantages are not shared by the more exact purely numerical approaches. In view of the ability of MO-IPT to access *both*, the selective-Mott incoherent metal and the Mott transition, we use it in this work. The technical details have already been worked out in detail in previous work³⁶, and we refer those interested in the details to these papers.

IV. RESULTS

We now describe our results. We choose t to have a non-interacting bandwidth $W = 3.0$ eV for the c_+ fermions. As mentioned, we denote the *net* JT coupling strength by λ . Assuming quasi-static JT distortions, the JT-term in H_{2D} is quadratic in the c_{\pm} , and is diagonalised along with the free part of the band structure to yield two bands

$$E_+(\mathbf{k}) = \epsilon_{\mathbf{k}} + \sqrt{(\epsilon_{\mathbf{k}} + 2q_1)^2 + 4q_2^2} \quad (2)$$

and

$$E_-(\mathbf{k}) = \epsilon_{\mathbf{k}} - \sqrt{(\epsilon_{\mathbf{k}} + 2q_1)^2 + 4q_2^2} \quad (3)$$

where q_1, q_2 are parameters chosen to be 0.05, 0.05 eV as representative values, with the understanding that their *renormalised* (by multi-orbital correlations and GdFeO₃

tilt) values will be very different, as we will show by explicit computation below. The local Hubbard U is chosen to be 3.0 eV, so that, with a $J_H = 0.7$ eV, we have $U' \simeq (U - 2J_H) = 1.7$ eV. The hopping strength is varied either by varying the GdFeO₃ tilt angle (θ) or strain. We keep in mind that, for the hopping between planar $x^2 - y^2$ orbital states, tensile strain is “equivalent” to enhanced octahedral tilt and reduced itinerance, while compressive strain corresponds to reduced tilt and enhancement of itinerance. Thus, as predicted in earlier sections, a strain-induced insulator-metal transition can be driven as a bandwidth-controlled Mott transition. Investigation into details of this Mott transition, however, throw up surprises we describe below in detail.

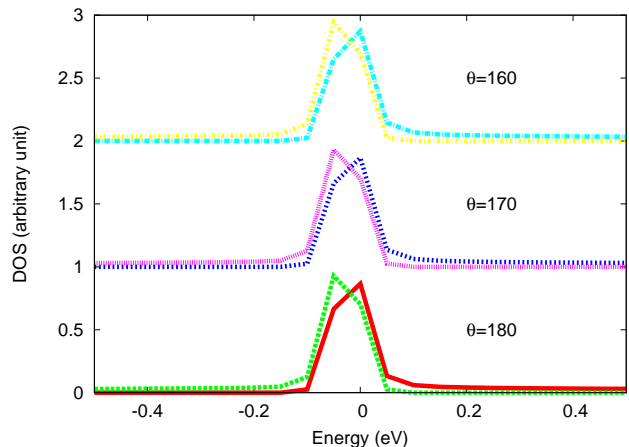


FIG. 1: (Color Online) Non-interacting DOS of the two bands (see text) for three different tilt angles θ mentioned in the figure. Red, blue and cyan represent the DOS of the $E_+(\mathbf{k})$ band at the three tilt angles shown and green, violet and yellow stand for the DOS of the $E_-(\mathbf{k})$ band at the same tilt angles respectively.

In Fig. 1, we show the tight-binding band (TBB) DOS with two bands $E_+(k, \theta)$, $E_-(k, \theta)$, and the corresponding one-electron DOS in the c_{\pm} basis as a function of θ , wherein the direct link between itinerance and octahedral tilt is manifest as a reduction of the TBB width with increasing tilt. The Fermi energy (E_F) is chosen to be at $\omega = 0$, defining a total band-filling, $n_t = n_{c,+} + n_{c,-}$. It is clear that the van-Hove singular (vHS) feature of the c_+ -fermion band is pinned to E_F , hinting at an intrinsic tendency toward instability to orbital density-wave (ODW) order, which could then *co-exist* with ferromagnetism. This could be reasoned within a weak-coupling, itinerant limit (small U, U'), as well as in the strong coupling regime. However, observation of half-metallic behavior, as in the CMR manganites, constrains one to use the latter route, as the strong $J_H (> W)$, implies even larger $U'U'$ from d -shell quantum chemistry. Generic observation of insulating or bad-metallic states in such systems is additional evidence for strong coupling physics. In this latter limit, one expects increasing importance

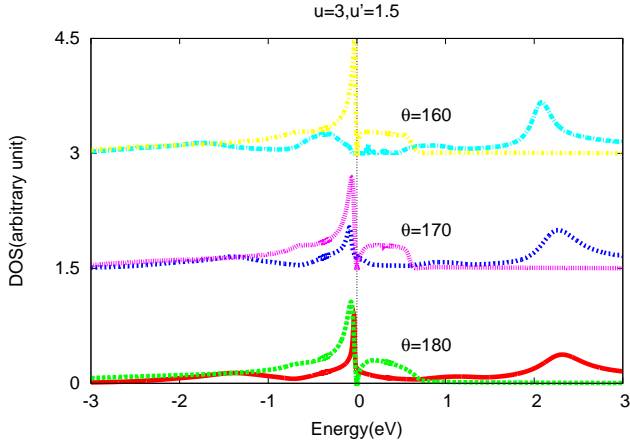


FIG. 2: (Color Online) DMFT DOS of the two bands for three different tilt angles θ , with intra-orbital Coulomb interaction $U = 3$, and inter-orbital Coulomb interaction $U_{ab} = 1.5$. The color codes of the DOS are the same as in Fig. 1.

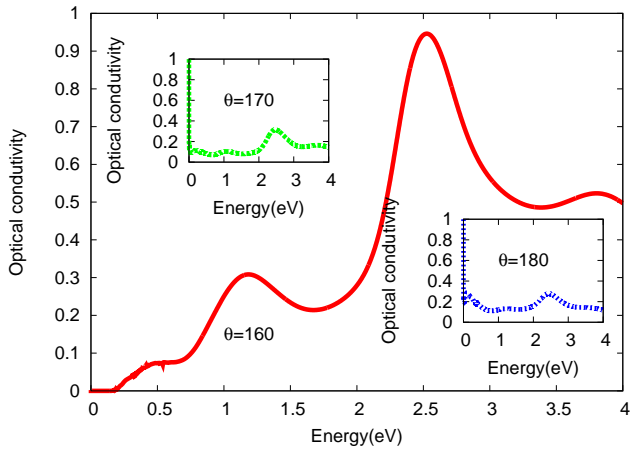


FIG. 3: (Color Online) Optical conductivity from DMFT calculations for different tilt angles θ (main panel $\theta=160^\circ$, right inset $\theta=180^\circ$, and left inset $\theta=170^\circ$).

of coupled orbital-spin superexchange processes, rather than the vHs, for instabilities toward ODW states. Finally, it is important to notice that the d -wave inter-band hybridization (in the original (a, b) fermions) is also reduced with increasing GdFeO_3 tilt: this will turn out to be useful later.

We now describe the effects of sizable local electronic correlations in detail. In Fig. 2, we show the orbital-resolved (DMFT) many-body density-of-states (DOS) as a function of θ . Several interesting features stand out clearly:

(i) for maximal $\theta = 180$, we find metallic behavior, though without LFL quasiparticles. Increasing GdFeO_3 tilt (reducing θ) reduces t , favoring increased (high-energy) incoherence, and the bad-metal undergoes a *continuous* Mott transition to a Mott-Hubbard insulator for

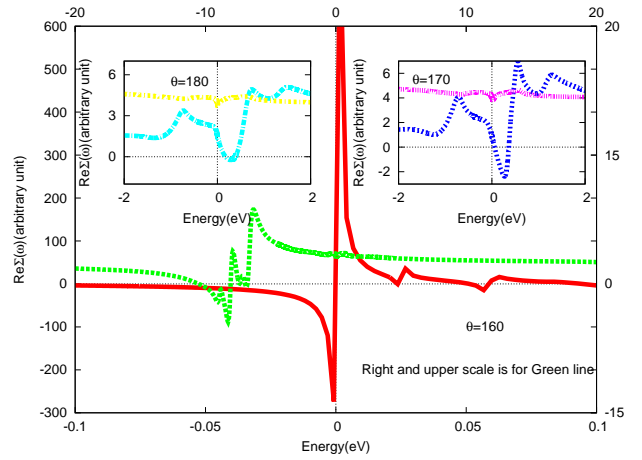


FIG. 4: (Color Online) (i) Real part of the DMFT self-energy at three different tilt angles (main panel $\theta=160^\circ$, right inset $\theta=170^\circ$, and left inset $\theta=180^\circ$). The different colors represent different bands as in Fig. 1.

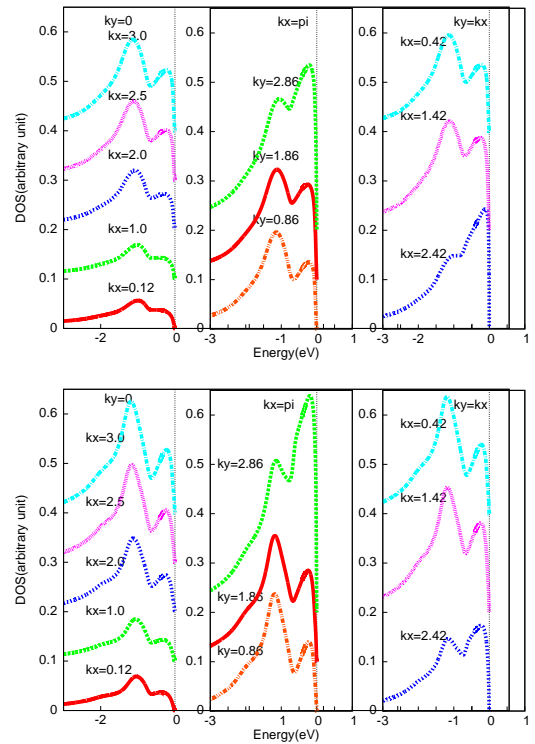


FIG. 5: (Color Online) The ARPES intensity at two different tilt angles (i) 180° and (ii) 170° , calculated along different directions of k_x and k_y in the Brillouin zone as shown.

$\theta = 160$. As surmised above, this is a band-width controlled Mott transition. Starting from the Mott insulator, increasing pressure now generically reduces θ , driving a continuous Mott transition to a bad-metal accompanied by reduction of the *renormalised* JT-distortion. Quite interestingly, precisely this is known to occur in LaMnO_3 under high pressure, and has been investigated by Held

*et al.*³⁵ within LDA+DMFT. We predict that a similar transition should obtain in bilayer manganites (or thin films) under suitable “pressure”.

(ii) In sharp contrast with the cubic manganites, however, the low- T (FM in the DE case with large J_H for mono- or bilayer manganites¹⁰) metallic state we find has no stable LFL quasiparticles. Rather, our DMFT spectra clearly show a low-energy continuum extending up to high energies $O(U)$. This means that the Green functions show branch-cut behavior, rather than a renormalised pole structure, in the complex energy plane. Remarkably, this non-LFL behavior (of the c_+ -band DOS) goes in tandem with a clear and strong tendency to (selective) Mott localisation of the c_- band (this is most clearly seen for the $\theta = 170$ result in Fig. 2). Examination of the orbital-resolved self-energies sheds more light on this phenomenon, as shown in Fig. 3: for the metallic cases ($\theta = 170, 180$), $\text{Re}\Sigma_+(\omega)$ shows sizably enhanced values near $E_F (= 0)$, implying heavily renormalised LFL quasiparticles, while $\text{Re}\Sigma_-(\omega)$ shows a clear kink at E_F , implying divergent effective mass. Correspondingly, $\text{Im}\Sigma_-(\omega) \simeq \omega^{(1-\eta)}$ with $\eta > 0$ at low energy, invalidating the LFL description of the metal. In the Mott insulator, $\text{Im}\Sigma_-(\omega)$ clearly shows the (expected) pole at $\omega = 0 (= E_F)$. Thus, our DMFT results describe an effective “two-fluid” situation, wherein Mott-localized c_- orbital states co-exist with (incoherent) “metallic” c_+ orbital states in the bad metal. This implies that though ODW-like states can be found in weak-coupling descriptions, the selective-Mott metal lies outside their scope, and only exists in the sizable correlation regime. Finally, the anomalous behavior of the propagators and self-energies can only arise as consequences of strong *dynamical* correlations, and are out of scope of LDA+U-type approximations.

(iii) In Fig. 5, we exhibit the DMFT one-particle spectral function, $A(\mathbf{k}, \omega) = (-1/\pi)\text{Im}G(|bfk, \omega)$ for two values of the GdFeO₃ tilt angle. The extinction of the quasi-coherent LFL pole in the one-particle Green function directly translates into (i) a power-law suppression in ARPES intensity as $\omega \rightarrow 0$. Due to the d -wave form factor of the inter-orbital hybridization (which enters the unperturbed band structure of the two-band model), this suppression is also \mathbf{k} -dependent: ARPES lineshapes show maximal suppression for \mathbf{k} along $(0, 0) - (0, \pi)$ and clear k -dependent anisotropy. This is a direct consequence of the complete suppression of the quasiparticle weight ($z_{FL} = 0$), as is clear from appearance of non-analyticities in $\text{Re}\Sigma(\omega = 0)$ (see Fig. 4). The fact that $G_-(k, \omega)$ now has *zeros* instead of poles at $\omega = 0$ also implies that the unperturbed Fermi surface undergoes a non-perturbative reconstruction: only the c_+ -fermions now contribute to the Luttinger count. (ii) As the GdFeO₃ tilt angle is reduced, a clear transfer of spectral weight to high energies shows up as appearance of a marked shoulder around $\Omega \simeq -2.0$ eV for $\theta = 170$ but not for $\theta = 180$. Its lack of momentum dependence, in strong contrast to that of the low-energy part, is in-

structive: reducing θ increases $U/t(\theta)$, transferring low-energy spectral weight to higher energy which, clearly, must be associated with dispersionless Hubbard band-like states. These observations are interesting in the context of studying latent electronic instabilities of TMO thin films: even in cases where the corresponding bulk systems show “uninteresting” paramagnetic metallic behavior⁴⁰, it may be possible to generate even analogues of high- T_c cuprates for thin films by appropriate strain tuning. Explicitly, metallic LaNiO₃ thin films with appropriate misfit strain have been theoretically predicted to lie close to Fermi surface instabilities. It is very conceivable that increase in effective U/t via manipulation of the tilt angle due to epitaxial constraints can produce an OSMT. If the reconstructed Fermi surface shows features propitious for electronic instabilities, a range of unconventional order(s) could result. Such a “strange” metallic phase as we find here, with associated topological Fermi surface reconstruction(s), would be quite interesting, since it would open up avenues for observation of exotic concepts like fractionalized Fermi liquid phases in TMO thin film and superlattices context.

(iv) The microscopic origin of the bad metallic behavior is revealed upon closer analysis: once the c_- -fermions are Mott-localized in DMFT, the effective problem is that of the c_+ -fermions scattering off Mott-localized c_- -fermion states. In the local “impurity” problem in DMFT, this maps *exactly* to the inverse of the seminal Anderson-Nozieres-de Dominicis x-ray-edge problem (this has been first recognized by Anderson in the context of the strange-metal phase in cuprates), wherein the infra-red power-law singular feature arises due to the “inverse” orthogonality catastrophe (OC). Now, $\text{Im}G_-(\omega) \simeq \theta(-\omega)|\omega|^{-(1-\eta)}$, in full accord with DMFT results. Identification with the X-ray edge problem has further interesting consequences. It implies that the local inter-orbital “excitonic” susceptibility also has infra-red power-law continuum behavior:

$$\begin{aligned} \text{Im}\chi_{+,-}(\omega) &= \int d\tau e^{i\omega\tau} \langle c_{\sigma,+}^\dagger c_{\sigma,-}(\tau); c_{\sigma,-}^\dagger c_{\sigma,+}(0) \rangle \\ &\simeq \theta(-\omega)|\omega|^{-(2\eta-\eta^2)} \end{aligned}$$

Hence, in the selective metal, orbital-excitons are not well-defined elementary excitations (as they would be if the metal were a LFL). Instead of the conventional long-lived particle-hole modes (i.e. a low energy coherent plasmon plus shake-up features at higher energy in the LFL), the low-energy spectrum is characteristic of a critical orbital *liquid*, in analogy with characterisation of spin-liquids: the particle-hole spectrum is a critical (power-law) continuum of “exciton-like” origin extending up to high energy. Thus, the (bosonic at long length scales) inter-orbital collective plasmon is infra-red unstable in the non-LFL metal, and the continuum feature in $\chi_{+,-}(\omega)$ strongly suggests charge-neutral *fermion-like* orbital excitations instead: this is the closest we can get to an orbital liquid with fermion-like elementary excitations

within DMFT. In fact, our finding of a selective-Mott metal is very similar to that of the FL* fractionalised liquid found in the context of f -electron metals by Senthil *et al.*⁶. In our case, the renormalised Fermi surface (FS) of the metallic orbital liquid now has a sharply defined sheet corresponding to the c_+ fermion band, while the c_- FS is “critical”. We thus dub our metal as an orbital FL* (OFL*) state, with asymptotically decoupled charge and orbiton excitations at low energy. This is very different from works where an orbital liquid state was proposed earlier on basis of slave-boson Hartree-Fock theories³⁷, where computing higher-order effects (beyond HF) of strongly coupled fermion-boson fluctuations present a formidable problem (in the absence of these, difficulties similar to those found in slave-particle approaches to the $t - J$ model are expected to arise). As in the FL* case, we expect that the OFL* state is stable at low but intermediate energy scales in $D = 2$, and instabilities to orbital-cum-magnetic ordered or LFL states will intervene at lower T to relieve its extensive degeneracy (finite entropy per site). Thus, ordered state(s) will arise directly from the non-LFL (“local” critical) metal, rather than from a band FS nesting-induced transition of a LFL, as would happen in the weak-coupling limit.

Onset of the OSMT also drastically transforms the bare band structure. In the correlated LFL (non-OSMT) phase of the two-band model, adiabatic continuity with the free Fermi gas implies that the traditional perturbative version of Luttinger’s theorem must hold. The renormalized Fermi surfaces are then identical (in shape and size) to that of the unperturbed two-band model, since the self-energies have no momentum dependence in DMFT. Once the OSMT occurs, however, appearance of the $\omega = 0$ pole in $\text{Im}\Sigma_-(\omega)$ implies that $\text{Im}G_{--}(k, \omega) = 0$ at $k = k_F, \omega = 0$. This causes a non-perturbative breakdown of adiabatic continuity, leading to wipe-out of LFL quasiparticles in the OFL* phase⁶. The resulting “Fermi surface” is now a critical one, corresponding to a modified Luttinger count of c_+ -fermions. An important consequence of this non-perturbative (topological, driven by wipe-out of the c_- Fermi surface by penetration of zeros of $G_{--}(k, \omega)$ in the OSMT phase to $\omega = 0$) Fermi surface reconstruction is that instabilities to orbital- and/or magnetically ordered phases can no longer be rationalized by appealing to possible nesting features of the unperturbed Fermi surface(s), since the one-to-one correspondence between the unperturbed and renormalized Fermi surfaces has been wiped out by onset of the OSMT. As increasingly appreciated³⁸, it is thus impossible to write down a traditional Ginzburg-Landau field theory by integrating out the *unperturbed* fermions, since these do not exist as stable elementary excitations any more. In fact, it is even impossible to write down a Luttinger-Ward functional when $\text{Im}\Sigma_-(\omega = 0)$ diverges, emphasizing that any instability to ordered states from such an anomalous metal must be truly unconventional.

The above Mott transition and OFL* state leave their characteristic fingerprint on one- and two-particle phys-

ical responses. In addition to anomalous continuum features in angle-resolved photoemission (ARPES), optical conductivity studies constitute a well-known spectroscopic diagnostic of two-particle response. In Fig. 4, we show the optical conductivity across the tilt-driven Mott transition above. Consistent with the small gap ($\Delta_{MH} \simeq 0.1$ eV) Mott insulator in Fig. 2 for $\theta = 160$, the optical conductivity, $\sigma(\omega)$, shows an onset from $\Omega = 2\Delta_{MH} \simeq 0.2$ eV, along with a mid-infrared feature and incoherent Hubbard band features at higher energy. The multiple Hubbard peaks arise from inter-orbital (U' , J_H) and intra-orbital (U) processes across the Hubbard bands in the Mott insulator. With reduction of the GdFeO₃ tilt, onset of (bad) metallicity is reflected in $\sigma(\omega)$ as a large scale transfer of high-energy spectral weight to low energies, on the scale of more than 4.0 eV, a characteristic fingerprint of Mottness. Additionally, no quasi-coherent Drude (LFL) peak is resolved in the spectra: instead, a low-energy pseudogap feature (with a mid-infrared hump) is clearly seen for $\theta = 170$. This evolves into an anomalous continuum with a slow fall-off in energy (and smeared mid-infrared feature) for $\theta = 180$, signalling increasing tendency toward low-energy coherence as the GdFeO₃ tilt is reduced. The marked absence of a quasi-coherent Drude response at low energy is a clear manifestation of the wipe-out of the lattice (LFL) coherence scale in the selective-Mott metal in DMFT. Thus, analysis of optical response of half-metallic and multi-orbital-based TMOs could be used to unearth the multi-orbital continuum at intermediate-but-low T . Optical studies of TMO thin films the U/t ratio in H) could confirm this trend in heterostructures: we predict that varying the A-cation in ABO₃ films will show the evolution of $\sigma(\omega)$ from Mott insulating to bad-metallic as the A-cation size is increased, e.g, changing the rare-earth (R) ion in RNiO₃ or doped RMnO₃ films from R=Ho to R=La across the lanthanide series.

Our work suggests that selective-Mottness, bad-metallicity and novel fractionalised excitations, hitherto features of theories for certain f -electron metals and cuprates, might be found “across the board” as orbital-FL* states in correlated TMOs. In particular, it is known that ARPES lineshapes and transport data for bilayer manganites show very “strange” features: ARPES lineshapes are anomalously broad, as in near-optimally doped cuprates, especially at temperatures higher than the orbital and magnetic ordering scales, and momentum-space (nodal-versus-anti-nodal) differentiation persists even above T_c^{FM} . It would be tempting to try and link such “strange” features to our proposed OFL* state. However, in spite of very close similarities to the FL* idea in Kondo-RKKY models, more formal field-theoretic work is needed to tease out the fractionalised orbitons in multi-orbital systems showing OSMT. This is beyond scope of the present work, and is left for future work.

V. EFFECTS OF STRAIN

The above results can now be readily used to gain qualitative insights into the effects of epitaxial strain on conduction states (metal-insulator, orbital-magnetic order) in TMO films grown on suitable substrates, e.g, $\text{LaNiO}_3/\text{LaAlO}_3$ (LNO/LAO) superlattice grown on a TiO_2 -terminated (001-face) SrTiO_3 substrate. We also qualitatively argue how competing (novel) ordered states may arise upon appropriate “strain engineering” in TMO thin films.

We begin by adapting our DMFT results and insights to a general model that is expected to hold for the system of an interface between a transition-metal oxide (manganites or LaNiO_3 , for example) on another transition-metal oxide substrate with ABO_3 structure but with slightly different lattice parameters (e.g, SrTiO_3). In such a simplified but very effective model⁴¹, the essentials can be recast in terms of energy balance at the interface between competing energies:

(i) the film cell parameters are constrained to fit those of the substrate. Since this implies bond elongation of film cell constants, it relaxes slowly. This constraint produces a unit-cell volume constraint: $V_{film} = V_{bulk}$, that appears as an elastic term in the free energy, given by $F_{el} = \frac{V}{2\kappa}(\frac{\delta V}{V})^2$. For LSMO on STO, this contribution is $O(0.015)$ eV⁴¹.

(ii) Due to epitaxial constraints (compressive or tensile strain affecting the inplanar hoppings, and the GdFeO_3 tilts at the interface), the electronic structure of the film undergoes drastic reconstruction, especially so in conditions realizing an OSMT, as described above. Let us consider the case where the hopping integral between the film and the substrate orbitals is affected by the renormalization of the electronic structure of the film. For example, for the LSMO/STO interface, this integral corresponds to the matrix element

$$t_{\perp} \simeq -\frac{t_{Mn,d_z^2,Ti,d_z^2}^2}{\epsilon_{Ti,d_z^2} - \epsilon_{Mn,d_z^2}} \quad (4)$$

where

$$t_{Mn,d_z^2,Ti,d_z^2} \simeq \frac{\langle d_{Mn,z^2} | p_{O,z} \rangle \langle p_{O,z} | d_{Ti,z^2} \rangle}{\epsilon_d - \epsilon_p}$$

. Owing to the short metal-oxygen distance ($\simeq 1.95A$), within LDA, this turns out to be $O(0.5)$ eV in a best qualitative estimate, while $(\epsilon_d - \epsilon_p) \simeq 1.5 - 2.0$ eV. Plugging these into t_{\perp} yields $t_{\perp} \simeq 0.125$ eV. Near an OSMT, however, there is a further drastic many-body renormalization due to the very small z_{FL} . If we take typical values for $z_{FL} = 0.05 - 0.1$, the renormalized t_{\perp} in a strongly correlated situation is now scaled down to 0.0125 eV (this is in contrast to the earlier estimate⁴¹, which gave a much larger $t_{\perp} \simeq O(0.1 - 0.5)$ eV).

These estimates now allow us to use this simple qualitative model to estimate the fate of the structural changes

at the interface. This is because one realizes the interfacial structure with $c < a$ if the elastic energy wins over the electronic delocalization energy, while another structure with $c > a$ obtains when the electronic delocalization energy exceeds the elastic energy. It is clear from (i),(ii) above that this is a rather delicate balancing act in interfaces made from strongly correlated systems. In particular, small changes in epitaxial constraints via strain tuning mentioned in the introduction can now easily tilt the balance between these two energies, leading to rather pronounced structural-cum-electronic changes at the interface. We detail upon this aspect below.

(i) Tensile strain ($e_{xy} > 0$) reduces the hopping via $t(e_{xy}) = t(1 - 2e_{xy})$. With increasing tensile strain, the correlated metal can thus be driven continuously to a Mott insulator. Further, since T-strain stabilizes the $x^2 - y^2$ relative to the $3z^2 - r^2$ orbital, it increases the tendency toward an effective one-band model in the less-than-or-equal to the quarter-filled case, with ferro-orbital order and antiferromagnetic spin order, as in the cuprates. This is borne out by an explicit calculation on a related but different model for manganites²⁵, which shows that $e_{xy} > 0$ increases the extent of the A -phase, reducing those of the FM and CE phases.

For not-too-large separation between the $x^2 - y^2$ and $3z^2 - r^2$ orbitals, the d -wave interband hybridisation gives rise to a novel possibility: it is conducive for observation of the exotic circulating current phase proposed by Varma for cuprates⁴², but with the circulating current patterns on three-site triangles connecting two in-plane O sites to the apical one^{43,44} if J_H is small. An important difference from the cuprates is that the $3z^2 - r^2$ orbital is now empty, rather than filled; nevertheless, for not-too-large $\delta = (\epsilon_{3z^2-r^2} - \epsilon_{x^2-y^2})$, the d -wave hybridisation in the two-band Hubbard model can populate the $3z^2 - r^2$ orbital and still give CC phases⁴⁴. While this fascinating proposal is presently intensively debated in the cuprate context, we propose that appropriate strain engineering might reveal its existence in e_g -orbital based TMO heterostructures. This mapping to an effective one-orbital model *with* an additional d -wave inter-orbital hybridisation in the tight-binding fit in the a, b basis has further novel consequences. In particular, multi-orbital, unconventional d -wave nematic order can also readily arise as a particle-hole condensate via a finite $\Delta_n = \sum_k (\cos k_x - \cos k_y) \langle a_{k\sigma}^\dagger b_{k\sigma} \rangle$. This will occur in a way similar to that found for the bilayer ruthenate $\text{Sr}_3\text{Ru}_2\text{O}_7$ ⁴⁵ and for underdoped Fe-arsenides⁴⁶. Additionally, a d -wave superconductor can also result as a particle-particle condensate with a finite $\Delta_{dsc} = \sum_k \gamma_{ab}(k) \langle a_{k\sigma}^\dagger b_{-k-\sigma}^\dagger \rangle$, where $\gamma_{ab}(k) = (\cos k_x - \cos k_y)$. Both these ordered states must result from the same microscopic interaction, and thus must be competing orders. In the non-LFL metal with infra-red singularities found in DMFT, these ordered states will result from a generalised Hartree-Fock (GHF) decoupling of the most relevant *residual* intersite two-particle interactions (since the one-electron mixing term (t_{ab}) in H_{2D} is irrelevant in the critical metal in the

absence of well-defined LFL quasiparticles). This residual two particle interaction is analogous to spin-orbital superexchange in Mott insulating phases, and is ipso-facto justified in the OSMT phase we find⁴⁷: $H_{res} = -(t_{ab}^2/(U' + J_H) \sum_{k,k',\sigma,\sigma'} \gamma_{ab}(k) \gamma_{ab}(k') a_{k\sigma}^\dagger b_{k\sigma} b_{k'\sigma'}^\dagger a_{k'\sigma'})$. Since this interaction scales like $1/D$ (with D the spatial dimensionality), a GHF decoupling indeed turns out to be *exact* within our DMFT.

(ii) Compressive strain ($e_{xy} < 0$) has exactly the reverse effect - it increases t and stabilizes the $3z^2 - r^2$ relative to the $x^2 - y^2$ orbital. Thus, a Mott-insulator to correlated (non-LFL) metal transition can be driven by increasing compressive strain. The situation for the ordered states is now more subtle, however. The stabilisation and preferential occupation of the $3z^2 - r^2$ orbitals implies favoring AF order in the bulk. This goes hand-in-hand with a reversal of the *net* “splitting”, $\delta = (\epsilon_{3z^2-r^2} - \epsilon_{x^2-y^2})$ from positive for $e_{xy} > 0$ to negative for $e_{xy} < 0$. Thus, viewed from the starting point of an unstrained system ($e_{xy} = 0$) with $\delta > 0$, C-strain produces, remarkably enough, an effective situation that corresponds to a system with a *negative* inter-orbital charge-transfer (CT) energy. This identification allows us to interpret the Mott transition in this case as one driven by “self-doping” a negative-CT insulator. Further, this situation also implies that the d -wave (nematic, SC) states discussed for T-strain now become unfavorable.

These are concrete examples of how strain engineering can sensitively affect the delicate balance between competing orders, and produce surprising features not to be found in the bulk. An exotic scenario would be where the balance between electronic delocalization energy and elastic energy can be tuned by strain engineering. This would make it conceivable, for example, to realize an unexpected outcome wherein a TMO thin film with $c > a$ can be “tuned” into a state with $c < a$ or vice-versa. In a multi-orbital system, this will drastically reconstruct the interfacial electronic structure, leading to emergence of ordered states not expected in the bulk. This is because $c > a$ and $c < a$ correspond to “tensile” and “compressive” strain which, as discussed above, lead to drastically different and novel outcomes for ordering instabilities at the interface via reconstruction of correlated electronic states.

Other observations may also be qualitatively rationalizable within our model study. For example, the experimental finding of a reduced conductivity and magnetic ordering scales in manganite thin films relative to their bulk values⁴⁸ is also naturally understood from our results. This arises from three factors, all of which conspire to produce an effective reduction in $t(\theta)$:

(i) reduction in lattice co-ordination number in the film relative to the bulk reduces screening of the Hubbard

U, U' , which increase as a result.

(ii) lattice mismatch at the interface reduces the $t(\theta)$ via tolerance factor and strain effects²⁵ effects, which acts like enhanced tilt relative to the bulk GdFeO₃ tilt.

(iii) larger $(U, U')/t(\theta)$ ratio implies selfconsistent enhancement of the net JT coupling via increased tendency toward localisation.

The consequent (self-consistent) reduction of $t(\theta)$ qualitatively explains lowered conductivity (increased localisation) as well as reduction in magnetic ordering scales, since $T_N^{af} \simeq 4t^2/(U' - J_H)$ and for FM, $T_c^{fm} \simeq t^2/J_H$ in the DE limit. Thus, as qualitatively alluded to in earlier sections, the structural DE and its interplay with conventional AH-DE is predicted to sensitively affect transport and magnetic ordering scales in TMO films in ways not always anticipated in the bulk case.

Finally, extension of our DMFT to multilayers requires consideration of the c -axis hopping (t_{ab}^{zz}), neglected in our $D = 2$ modelling. Baena *et al.*²⁵ have considered this aspect in detail in a related model for manganites. How these effects will affect physical properties in response to external stimuli and affect the interplay of competing ordered states within remains an open issue of great interest in the TMO heterostructure context.

VI. CONCLUSION

In conclusion, we have considered the detailed effect of the GdFeO₃ tilt, ubiquitous in TMO systems. Using the two-orbital Hubbard model as a template, we have identified a new feature, namely, that this tilt acts like a *structural* “reverse double exchange” in the orbital sector. It thus acts contrary to the Anderson-Hasegawa (magnetic) double exchange, and the competition between these two DE processes is shown to be a generically relevant feature in TMOs. This additional control parameter is attractive in the sense of not causing (doping induced) disorder, and can be continuously tuned by suitable choice of substrate and strain engineering. Adopting a strong correlation view of TMO, this parameter sensitively affects carrier itinerance, inducing phase transitions between Mott insulators and incoherent metals with ill-defined LFL quasiparticles. This breakdown of the LFL metal arises from the orbital-selective character of the Mott transition, and we argue that this is an orbital-FL* state with fractionalised orbitons. As a particularly attractive fall-out of our work, suitable strain engineering is also predicted to generate situations conducive to novel ordered states, whose further exploration is undoubtedly of great topical interest. A detailed study of this last aspect is left for future consideration.

¹ M. Imada, et al., J. Phys.: Condens. Matter **22**, 164206 (2010).

² P.W. Anderson, *Nature Phys.* **2**, 626 (2006).

- ³ E Dagatto, Nanoscale phase separation and colossal magnetoresistance, *Springer* (2003).
- ⁴ I. A. Sergienko, C. Sen, and E. Dagotto, *Phys. Rev. Lett.* **97**, 227204 (2006).
- ⁵ L Craco, et al., *Phys. Rev. B* **79**, 075125 (2009).
- ⁶ T. Senthil et al., *Phys. Rev. Lett.* **90**, 216403 (2003).
- ⁷ J van den Brink *Physica B* 312-313, 743-744 (2002).
- ⁸ R Takahashi et al., *Appl. Phys. Lett.* **96**, 192111 (2010).
- ⁹ M Kareev et al., *Appl. Phys. Lett.* **93**, 061909 (2008).
- ¹⁰ T. Maitra and A. Taraphder, *EPL* **65**, 262 (2004).
- ¹¹ P. Dey, T. K. Nath and A. Taraphder, *Appl. Phys. Lett.* **91**, 012511 (2007).
- ¹² J. B. Goodenough, Magnetism and the Chemical Bond (Wiley Interscience, New York, 1963)
- ¹³ Y. Suzuki, et al., *J. Appl. Phys.* **83**, 7064 (1998).
- ¹⁴ G. Maris, V. Volotchaev and T.T.M Palstra, *New Journal of Physics* **6**, 153 (2004).
- ¹⁵ M. K. Stewart, et al., *Phys. Rev. B* **83**, 075125 (2011).
- ¹⁶ J. Kanamori, *J. Appl. Phys.* **31**, 14S (1960).
- ¹⁷ F Masee, et al., *Nature Physics* **7**, 978982 (2011).
- ¹⁸ V. Ferrari et al., *Modern Physics Letters B*, Vol. 15, No. 23 (2001) 10311040
- ¹⁹ N Furukawa, arXiv:cond-mat/9505011.
- ²⁰ N. D. Mathur, and P. B. Littlewood, *Solid State Commun.* **119**, 271 (2001).
- ²¹ K Byczuk et al., *Phys. Rev. Lett.* **94**, 056404 (2005).
- ²² P. W. Anderson and H Hasegawa *Phys. Rev.* **100**, 675681 (1955).
- ²³ S. A. Wolf, D. D. Awschalom, R. A. Buhrman, J. M. Daughton, S. von Molnr, M. L. Roukes, A. Y. Chtchelkova, and D. M. Treger, *Science* **294**, 1488 (2001).
- ²⁴ J chakhalian *Science* **314**, 1114 (2007).
- ²⁵ A. Baena, et al., *Phys. Rev. B* **83**, 064424 (2011).
- ²⁶ L Craco, et al., arXiv:cond-mat/0110229 (2001).
- ²⁷ J. K. Freericks and V. Zlatić *Rev. Mod. Phys.* **75**, 13331382 (2003).
- ²⁸ M.S. Laad et al., *Phys. Rev. Lett.* **91**, 156402 (2003).
- ²⁹ K. Haule and G. Kotliar, *Phys. Rev. B* **76**, 104509 (2007).
- ³⁰ D. E. Logan and N. L. Dickens *Europhys. Lett.* **54** 227 (2001).
- ³¹ C. A. Perroni, et al., *Phys. Rev. B* **75**, 045125 (2007).
- ³² E Gull, et al., *Rev. Mod. Phys.* **83**, 349404 (2011).
- ³³ R. Bulla, et al., *Rev. Mod. Phys.* **80**, 395450 (2008).
- ³⁴ A Georges, et al., *Rev. Mod. Phys.* **68**, 13-125 (1996).
- ³⁵ K Held, et al., *Int. J. Mod. Phys. B* **15**, 2611 (2001)
- ³⁶ M S Laad et al., *J Phys. Condens. Matter* **24**, 232201 (2012).
- ³⁷ J van den Brink, et al., arXiv:cond-mat/0206053.
- ³⁸ K B. Dave et al., *Phys. Rev. Lett.* **110**, 090403 (2013).
- ³⁹ J. Tomczak and S. Biermann, *Phys. Rev. B* **80**, 085117 (2009).
- ⁴⁰ H. K. Yoo et al., *Sci. Rep.* **5**, 8746; DOI:10.1038/srep08746 (2015).
- ⁴¹ Marie-Bernadette Lepetit et al., *Phys. Rev. Lett.* **108**, 087202 (2012)
- ⁴² C. M. Varma *Phys. Rev. B* **73**, 155113 (2006).
- ⁴³ C. Weber et al., *PRL* **102**, 017005 (2009).
- ⁴⁴ M S Laad, et al., arXiv:0902.1903.
- ⁴⁵ W. Wu, et al., *Phys. Rev. B* **83**, 045106 (2011).
- ⁴⁶ Chu, et al., *Science* **337**, 710 (2012).
- ⁴⁷ M. S. Laad et al., *Phys. Rev. Lett.* **103**, 017002 (2009)
- ⁴⁸ P Orgiani, et al., *Phys. Rev. B* **76**, 012404 (2007).